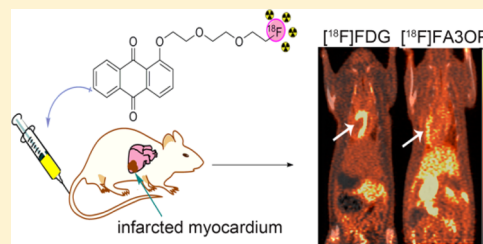


Novel  $^{18}\text{F}$ -Labeled 1-Hydroxyanthraquinone Derivatives for Necrotic Myocardium ImagingAi-Yan Ji,<sup>†,‡,§</sup> Qiao-Mei Jin,<sup>‡,§</sup> Dong-Jian Zhang,<sup>‡,§</sup> Hua Zhu,<sup>||</sup> Chang Su,<sup>†,‡,§</sup> Xing-Hua Duan,<sup>†,‡,§</sup> Li Bian,<sup>‡,§,⊥</sup> Zi-Ping Sun,<sup>∇</sup> Yi-Cheng Ni,<sup>‡,§,#</sup> Jian Zhang,<sup>\*,‡,§</sup> Zhi Yang,<sup>\*,||</sup> and Zhi-Qi Yin<sup>\*,†</sup><sup>†</sup>Department of Natural Medicinal Chemistry & Jiangsu Key Laboratory of Natural Medicines, China Pharmaceutical University, Nanjing 210009, Jiangsu, China<sup>‡</sup>Laboratories of Translational Medicine, Jiangsu Province Academy of Traditional Chinese Medicine, Nanjing 210028, Jiangsu, China<sup>§</sup>Affiliated Hospital of Integrated Traditional Chinese and Western Medicine, Nanjing University of Chinese Medicine, Nanjing 210028, Jiangsu, China<sup>||</sup>Key Laboratory of Carcinogenesis and Translational Research, Department of Nuclear Medicine, Peking University Cancer Hospital & Institute, Beijing 100142, China<sup>⊥</sup>College of Pharmacy, Nanjing University of Chinese Medicine, Nanjing, Jiangsu 210023, China<sup>∇</sup>Radiation Medical Institute, Shandong Academy of Medical Sciences, Jinan 250062, Shandong, China<sup>#</sup>Theranostic Laboratory, Campus Gasthuisberg, KU Leuven, 3000 Leuven, Belgium

## S Supporting Information

**ABSTRACT:** Rapid detection and precise evaluation of myocardial viability is necessary to aid in clinical decision making whether to recommend revascularization for patients with myocardial infarction (MI). Three novel  $^{18}\text{F}$ -labeled 1-hydroxyanthraquinone derivatives were synthesized, characterized, and evaluated as potential necrosis avid imaging agents for assessment of myocardial viability. Among these tracers, [ $^{18}\text{F}$ ]FA3OP emerged as the most promising compound with best stability and highest targetability. Clear PET images of [ $^{18}\text{F}$ ]FA3OP were obtained in rat model of myocardial infarction and reperfusion at 1 h after injection. In addition, the possible mechanisms of [ $^{18}\text{F}$ ]FA3OP for necrotic myocardium were discussed. The results showed [ $^{18}\text{F}$ ]FA3OP may bind DNA to achieve targetability to necrotic myocardium by intercalation. In summary, [ $^{18}\text{F}$ ]FA3OP was a more promising “hot spot imaging” tracer for rapid visualization of necrotic myocardium.

**KEYWORDS:** Myocardial infarction, necrosis avid agents, anthraquinone,  $^{18}\text{F}$ , positron emission tomography



In clinical practices, timely myocardial revascularization is recognized as the most effective therapy for myocardial infarction (MI) to salvage reversible myocardium. However, it is not suitable for all MI patients. Related studies show that the survival of patients who have little reversibly viable myocardium in the MI area was significantly decreased after revascularization.<sup>1</sup> Thus, it is essential to assess myocardial viability before revascularization to guide clinical intervention.

Necrosis avid agents (NAAs) could selectively localize in nonviable infarct myocardium, which may be helpful for the assessment of myocardial viability and prognosis.<sup>2</sup> Currently, there are no FDA-approved infarct avid imaging agents for evaluating myocardial vitality within the time frame necessary to direct decisions for early revascularization therapy to achieve maximal myocardial salvage (the window for maximal patient benefit from thrombolytic therapy is within the first 6 h of chest pain<sup>3</sup>). Therefore, developing probes for fast and accurate imaging of necrotic myocardium is particularly important.

Our group has been focusing on infarct avid agents for the fast imaging of necrotic myocardium. Hypericin (Hyp), a

dimeric anthraquinone compound, is regarded as a powerful naturally occurring necrosis avid agent (NAA).<sup>4,5</sup> In previous studies, radioiodine-labeled Hyp showed high affinity for necrotic myocardium in reperfused MI models.<sup>4</sup> However, the long plasma half-life and high blood pool activity make it impossible for early in vivo visualization of necrotic myocardium.<sup>5,6</sup> To seek for superior necrosis avid agents in imaging, we further evaluated the necrosis targetability of monomeric anthraquinones. The results showed that monomeric anthraquinones exhibited necrosis targetability and shorter plasma half-life times.<sup>7</sup> Considering their excellent pharmacokinetic properties, monomeric anthraquinone(s) would be used as vehicles of infarct avid imaging agents for visualizing necrotic myocardium at early time points.

Currently, positron emission tomography (PET) has been widely used due to its superiority to single photon emission

**Received:** October 10, 2016

**Accepted:** December 28, 2016

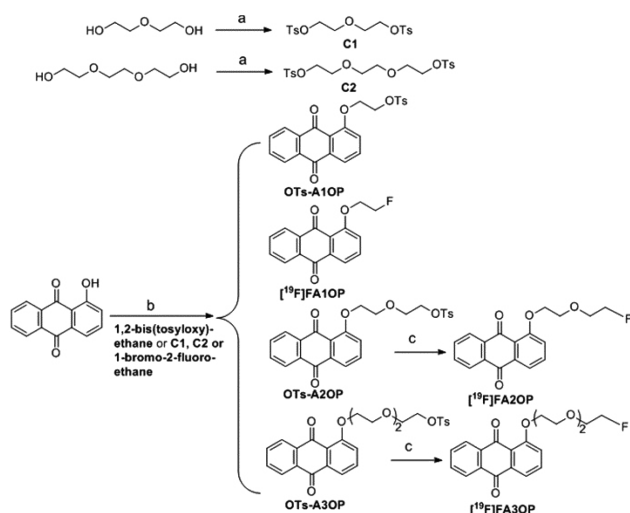
**Published:** December 28, 2016



computed tomography (SPECT) in spatial resolution, high sensitivity, and accurate attenuation correction. In addition,  $^{18}\text{F}$ -labeled tracers, with their longer half-life, would facilitate clinical protocols.<sup>8</sup> Herein,  $^{18}\text{F}$  and monomeric anthraquinone(s) were chosen to build necrosis avid probes. In addition, in order to improve tracers' blood clearance in vivo, we introduced hydrophilic polyethylene glycol (PEG) into monomeric anthraquinone(s) for exploring the potential of rapid visualization of necrosis myocardium.

The synthesis route<sup>9,10</sup> of tosylate precursors and non-radioactive reference compounds was shown in Scheme 1. All key compounds were analyzed by  $^1\text{H}$  and  $^{13}\text{C}$  NMR spectroscopy and ESI high-resolution mass spectroscopy to confirm the identity.

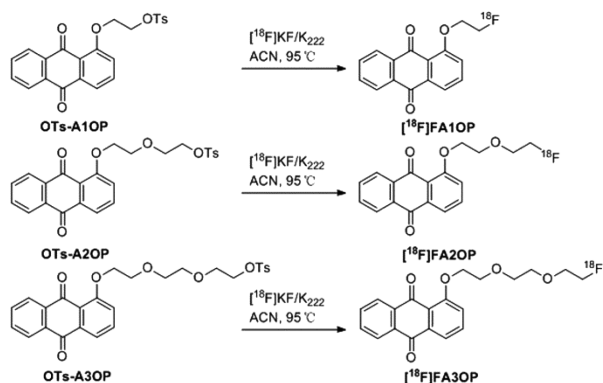
**Scheme 1. Synthesis Route of Tosylate Precursors and Nonradioactive References [ $^{19}\text{F}$ ]FA1OP, [ $^{19}\text{F}$ ]FA2OP, and [ $^{19}\text{F}$ ]FA3OP<sup>a</sup>**



<sup>a</sup>Reagents and conditions: (a) TsCl, KOH,  $\text{CH}_2\text{Cl}_2$ , 0 °C; (b) DMF, NaH, rt to 40 °C; (c) TBAF (1.0 M in THF), THF, 70 °C.

The labeling procedures of [ $^{18}\text{F}$ ]FA1OP, [ $^{18}\text{F}$ ]FA2OP, and [ $^{18}\text{F}$ ]FA3OP have been shown in Scheme 2. The total reaction time was within 90 min, and the overall radiochemical yield was approximately 15–20% (no decay corrected,  $n = 3$ ).

**Scheme 2. Radiolabeling Routes of [ $^{18}\text{F}$ ]FA1OP, [ $^{18}\text{F}$ ]FA2OP, and [ $^{18}\text{F}$ ]FA3OP<sup>a</sup>**



<sup>a</sup>ACN = acetonitrile; K<sub>222</sub> = Kryptofix2.2.2.; KF = potassium fluoride.

The specific (radio)activity was about  $72.25 \pm 14\%$  GBq/ $\mu\text{mol}$  ( $n = 4$ ). Quality control of [ $^{18}\text{F}$ ]FA1OP, [ $^{18}\text{F}$ ]FA2OP, and [ $^{18}\text{F}$ ]FA3OP were performed with HPLC analyses (Figure 1 and Figure S2).

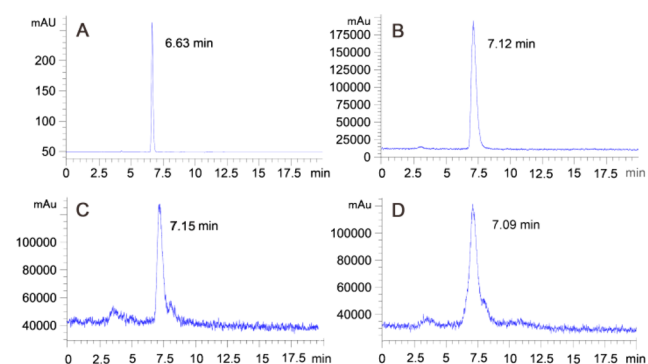


**Figure 1.** [ $^{19}\text{F}$ ]FA3OP (A) and [ $^{18}\text{F}$ ]FA3OP (B). Profiles of stability study of [ $^{18}\text{F}$ ]FA3OP after incubation in rat serum at 37 °C for 6 h (C) and in 80% ethanol solution for 5 h (D).

The radiochemical purity was >95%. The octanol–PBS distribution coefficient (Log P) of  $^{18}\text{F}$ -hydroxyanthraquinone derivatives were 1.21, 1.02, and 0.87 for [ $^{18}\text{F}$ ]FA1OP, [ $^{18}\text{F}$ ]FA2OP, and [ $^{18}\text{F}$ ]FA3OP, respectively. The hydrophilicity of tracers increased with the extension of polyethylene glycol chain. The HPLC profiles of stability studies are shown in Figure 1 and Figure S2. After storage in 80% ethanol solution at room temperature for 1 h, 66% of [ $^{18}\text{F}$ ]FA1OP was intact. Other tracers are stable during at least a 5 h period. For the radiotracers incubated in rat serum at 37 °C for 1 h, only about 10% of [ $^{18}\text{F}$ ]FA1OP was intact. However, other tracers are stable during at least a 6 h period in rat serum. Therefore, in the studies performed afterward, the relatively stable [ $^{18}\text{F}$ ]FA2OP and [ $^{18}\text{F}$ ]FA3OP were selected for further evaluation.

Bearing in mind that an aim of this work was to investigate the targetability to necrotic tissues of  $^{18}\text{F}$ -hydroxyanthraquinone derivatives, a set of biological studies were carefully designed. The biologic distribution results in mice model of muscular necrosis are shown in Table S1. The two tracers showed different necrosis targetability in vivo. The necrotic uptake and radioactivity ratio of [ $^{18}\text{F}$ ]FA3OP was higher than [ $^{18}\text{F}$ ]FA2OP at three time points ( $p < 0.05$ ). As described in Table S1, the clearance of [ $^{18}\text{F}$ ]FA3OP from normal organs was favorable for imaging. The results obtained from the biodistribution study encouraged us to further evaluate [ $^{18}\text{F}$ ]FA3OP by in vivo microPET/CT imaging in rats with MI.

Representative PET-CT images of control rats and model rats of MI/R at 1 h after administration of [ $^{18}\text{F}$ ]FDG or [ $^{18}\text{F}$ ]FA3OP are shown in Figure 2. PET/CT showed that the outline of the heart was clear (Figure 2A1) and that obvious uptake defect in infarct region was observed in model rats (Figure 2A3) after intravenous injection [ $^{18}\text{F}$ ]FDG. Figure 2A4 reveals a high radioactivity uptake of [ $^{18}\text{F}$ ]FA3OP in necrotic myocardium compared with the control rat (Figure 2A2). A perfect match between uptake defect area of [ $^{18}\text{F}$ ]FDG and area of high [ $^{18}\text{F}$ ]FA3OP uptake on PET is seen (Figure 2A3,A4). The results of PET/CT imaging demonstrated a selective accumulation of [ $^{18}\text{F}$ ]FA3OP in necrotic myocardium.

The ratio necrotic myocardium/viable myocardium obtained following i.v. injection of [ $^{18}\text{F}$ ]FA3OP into model rats was shown in Figure 2B. Injection of [ $^{18}\text{F}$ ]FA3OP to model rats

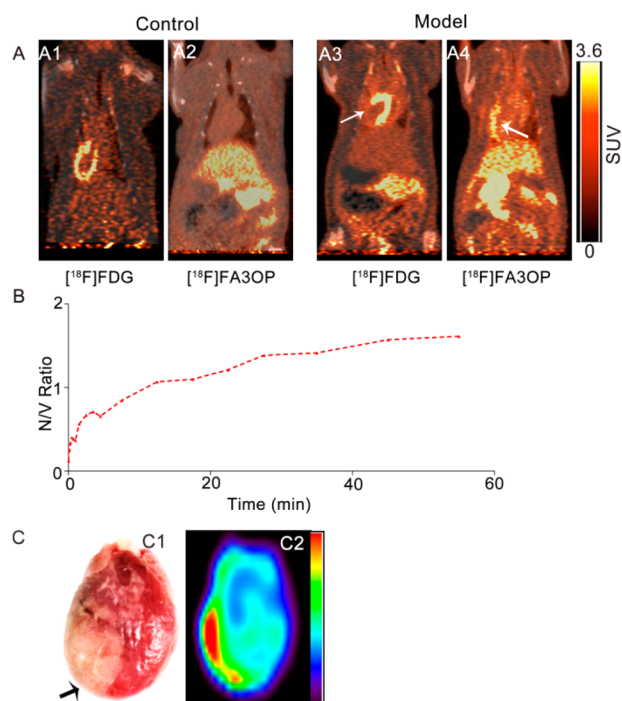


**Figure 2.** Representative PET/CT images of control rats and model rats of MI/R at 1 h after administration of [ $^{18}\text{F}$ ]FDG (A1,A3) and [ $^{18}\text{F}$ ]FA3OP (A2,A4). (B) Ratio necrotic myocardium/viable myocardium of [ $^{18}\text{F}$ ]FA3OP in a MI/R rat. V = viable myocardium, N = necrotic myocardium. (C) Post-mortem analyze of isolated heart from model rats of [ $^{18}\text{F}$ ]FA3OP: the digital photographs of TTC staining image of whole heart (C1) and representative PET image of isolated heart (C2). Arrows indicate the location of necrotic myocardium.

resulted in distinct accumulation of radioactivity around the damaged area of the left ventricular lateral wall (Figure S4). The SUVs in the infarcted myocardium were higher than those measured for the viable myocardium of the same animals from 20 min postinjection, with a highest SUV ratio of 1.61 between the damaged and the healthy walls at 1 h postinjection, which is consistent with the PET imaging time window.

We further proved the presence of necrotic tissues with enzymatic histochemical staining using TTC. On the TTC-stained heart (Figure 2C1), the infarcted myocardium remained pale, whereas viable myocardium was stained brick red. A homogeneous high radioactivity uptake (in red) only occurred in the infarcted areas on PET image of isolated heart (Figure 2C2), which corresponded well to the pale region on TTC stained specimen.

During myocardial infarction (MI), necrosis of myocardial cells releases large amounts of DNA, representing a potential target for molecular imaging of necrotic myocardium.<sup>11</sup> Research suggested that hocheist-IR<sup>12</sup> and Gd-To<sup>13</sup> can image necrotic tissue of myocardial infarction by binding to exposed DNA (E-DNA). Meanwhile, anthraquinone with a planar tricyclic structure is the backbone of many known antitumor drugs like doxorubicin capable of targeting at the molecular/DNA level.<sup>14</sup> Thus, we speculated that anthraquinone-based radiotracers may bind to E-DNA for necrotic myocardium imaging. The binding mechanism on the reaction of [ $^{19}\text{F}$ ]FA3OP with DNA was investigated by UV–visible spectrophotometry and fluorescence quenching technique in vitro. The results were shown in Figure 3.

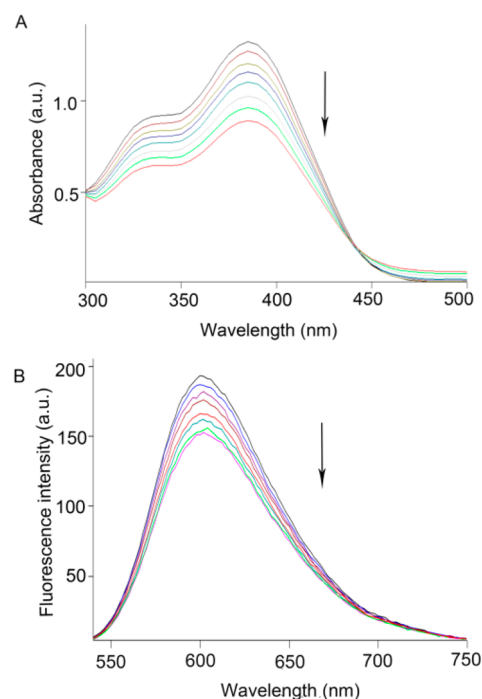


**Figure 3.** Absorption spectra of [ $^{19}\text{F}$ ]FA3OP in the absence and presence of increasing amounts of DNA at room temperature in Tris–HCl buffer (pH = 7.35). The arrow shows the absorbance change upon increasing the DNA concentration (A). Emission spectra of EB bound to DNA in the presence of [ $^{19}\text{F}$ ]FA3OP (B). The arrow shows the intensity changes upon increasing the compound concentration.

When a small molecule interacts with DNA and forms a complex, changes in absorbance and in the position of the absorption maximum occurs. Hypochromism was generated through an intercalative mode of binding between an aromatic chromophore and the base pairs of DNA.<sup>15</sup> When increasing concentration of DNA was continuously added to the solution, hypochromism was observed on [ $^{19}\text{F}$ ]FA3OP and Ct-DNA interaction. The percentage of hypochromism was found to be 32.6% from spectral titration. The DNA binding constant ( $K_b$ ) was  $2.2 \times 10^3 \text{ M}^{-1}$ . This indicated that [ $^{19}\text{F}$ ]FA3OP may bind to Ct-DNA by intercalation mode. The results are shown in Figure 3A.

The binding of [ $^{19}\text{F}$ ]FA3OP with Ct-DNA was studied by evaluating the fluorescence emission intensity of the EB–DNA system upon successive addition of the [ $^{19}\text{F}$ ]FA3OP, which acted as quencher. When [ $^{19}\text{F}$ ]FA3OP was added into the EB–DNA solution, fluorescence intensity decreased regularly. The  $K_{SV}$  value for [ $^{19}\text{F}$ ]FA3OP was  $1.60 \times 10^4 \text{ mol}^{-1}$ . This suggested that the partial replacements of EB bound to DNA by the [ $^{19}\text{F}$ ]FA3OP and [ $^{19}\text{F}$ ]FA3OP binds to DNA in intercalative mode, which is consistent with the result of UV–visible absorption spectroscopy. The results are shown in Figure 3B. According to the results of spectroscopy, [ $^{19}\text{F}$ ]FA3OP may be interacting with DNA for targeting necrotic tissues. However, the interaction behavior between them has not been investigated in vivo. Thus, the necrosis avidity mechanism of [ $^{19}\text{F}$ ]FA3OP needs to be explored further in following experiments.

Potential reversibility of myocardium is an important consideration in CAD patients when being considered for revascularization. [ $^{18}\text{F}$ ]FDG has been considered the gold standard for detection of the reversibility of injured



myocardium with PET.<sup>16</sup> However, FDG uptake is influenced by confounding factors such as individual differences and myocardial inflammation of infarcted region, which often leads to false negatives and positives.<sup>17</sup> The use of radiolabeled necrosis-avid probes may provide depiction of infarcted myocardium to guide clinical decision-making. Compared with [<sup>18</sup>F]FDG, necrosis-avid tracers have the following advantages. First, they were designed with high avidity and specificity; second, they were not affected by individual differences and inflammation. Furthermore, imaging necrosis can avoid functional impairment of salvageable myocardium caused by the absorption of tracers. Moreover, it may allow evaluation of patient follow-up and outcome assessment of revascularization therapies. To the best of our knowledge, this is the first attempt to label anthraquinone derivatives with <sup>18</sup>F and explore their targetability to necrotic tissues and imaging necrotic myocardium in vivo by PET. Furthermore, the possible mechanisms of [<sup>18</sup>F]FA3OP for necrotic myocardium were discussed. [<sup>19</sup>F]FA3OP may bind DNA to achieve targetability to necrotic myocardium by intercalation in vitro. In summary, [<sup>18</sup>F]FA3OP is a promising agent for fast imaging of necrotic myocardium.

## ■ ASSOCIATED CONTENT

### ● Supporting Information

The Supporting Information is available free of charge on the ACS Publications website at DOI: 10.1021/acsmedchemlett.6b00398.

Details regarding materials and methods, chemistry, radiochemistry, octanol–water partition coefficient, in vitro stability study, animal models, microPET protocols, and interaction with DNA (PDF)

## ■ AUTHOR INFORMATION

### Corresponding Authors

\*E-mail: [zjwonderful@hotmail.com](mailto:zjwonderful@hotmail.com).

\*E-mail: [pekyz@163.com](mailto:pekyz@163.com).

\*E-mail: [chyzq2005@126.com](mailto:chyzq2005@126.com).

### ORCID

Jian Zhang: 0000-0002-8402-9753

### Author Contributions

A.-Y.J., Q.-M.J., Y.-C.N., J.Z., Z.Y., and Z.-Q.Y. have designed the studies. A.-Y.J., C.S., L.B., and X.-H.D. have done the biological experiments. A.-Y.J., Q.-M.J., D.-J.Z., and H.Z. have performed the chemistry work. All the aforementioned authors and Z.-P.S. have participated in preparing, editing, and approving the content of the manuscript.

### Funding

This work was partially supported by the National Natural Science Foundation of China (No. 81501536, 81473120), A Project Funded by the Priority Academic Program Development of Jiangsu Higher Education Institutions, and A Project of Medical and Health Technology Development Program in Shandong Province (No.2013WS0354).

### Notes

The authors declare no competing financial interest.

## ■ ACKNOWLEDGMENTS

We thank Mrs Shaoli Song for her generous help.

## ■ ABBREVIATIONS

MI/R, myocardial infarction and reperfusion; NAAs, necrosis avid agents; Hyp, hypericin; SPECT, single photon emission computed tomography; PET, positron emission tomography; PEG, polyethylene glycol; RP-HPLC, reversed-phase high performance liquid chromatography; Ct-DNA, calf thymus DNA; EB, ethidium bromide; <sup>18</sup>F-FDG, fluorine-18 deoxyglucose

## ■ REFERENCES

- (1) Allman, K. C.; Shaw, L. J.; Hachamovitch, R.; Udelson, J. E. Myocardial viability testing and impact of revascularization on prognosis in patients with coronary artery disease and left ventricular dysfunction: a meta-analysis. *J. Am. Coll. Cardiol.* **2002**, *39*, 1151–1158.
- (2) Cona, M. M.; Oyen, R.; Ni, Y. C. Necrosis Avidity of Organic Compounds: a Natural Phenomenon with Exploitable Theragnostic Potentials. *Curr. Med. Chem.* **2015**, *22*, 1829.
- (3) Khaw, B. A. The current role of infarct avid imaging. *Semin. Nucl. Med.* **1999**, *29*, 259–270.
- (4) Van de Putte, M.; Wang, H. J.; Chen, F.; de Witte, P. A.; Ni, Y. C. Hypericin as a marker for determination of tissue viability after intratumoral ethanol injection in a murine liver tumor model. *Acad. Radiol.* **2008**, *15*, 107–113.
- (5) Fonge, H.; Vunckx, K.; Wang, H. J.; Feng, Y. B.; Mortelmans, L.; Nuyts, J.; Bormans, G.; Verbruggen, A.; Ni, Y. C. Non-invasive detection and quantification of acute myocardial infarction in rabbits using mono-[<sup>123</sup>I] iodohypericin  $\mu$ SPECT. *Eur. Heart J.* **2008**, *29*, 260–269.
- (6) Feng, Y. B.; Cona, M. M.; Vunckx, K.; Li, Y.; Chen, F.; Nuyts, J.; Gheysens, O.; Zhou, L.; Xie, Y.; Oyen, R.; Ni, Y. C. Detection and quantification of acute reperfused myocardial infarction in rabbits using DISA-SPECT/CT and 3.0T cardiac MRI. *Int. J. Cardiol.* **2013**, *168*, 4191–4198.
- (7) Wang, Q.; Yang, S. W.; Jiang, C. H.; Li, J. D.; Wang, C.; Chen, L. W.; Jin, Q. M.; Song, S. L.; Feng, Y. B.; Ni, Y. C.; Zhang, J.; Yin, Z. Q. Discovery of Radioiodinated Monomeric Anthraquinones as a Novel Class of Necrosis Avid Agents for Early Imaging of Necrotic Myocardium. *Sci. Rep.* **2016**, *6*, 21341.
- (8) Pimlott, S. L.; Sutherland, A. Molecular tracers for the PET and SPECT imaging of disease. *Chem. Soc. Rev.* **2011**, *40*, 149–162.
- (9) Bongers, K. M.; van den Berg, R. J.; Heitman, L. H.; IJzerman, A. P.; Oosterom, J.; Timmers, C. M.; Overkleeft, H. S.; van der Marel, G. A. Synthesis and evaluation of homo-bivalent GnRHR ligands. *Bioorg. Med. Chem.* **2007**, *15*, 4841–4856.
- (10) Cui, M. C.; Wang, X. D.; Yu, P. R.; Zhang, J. M.; Li, Z. J.; Zhang, X. J.; Yang, Y. P.; Ono, M.; Jia, H. M.; Saji, H.; Liu, B. L. Synthesis and evaluation of novel <sup>18</sup>F labeled 2-pyridinylbenzoxazole and 2-pyridinylbenzothiazole derivatives as ligands for positron emission tomography (PET) imaging of beta-amyloid plaques. *J. Med. Chem.* **2012**, *55*, 9283–9296.
- (11) Khan, R. S.; Martinez, M. D.; Sy, J. C.; Pendergrass, K. D.; Che, P. L.; Brown, M. E.; Cabigas, E. B.; Dasari, M.; Murthy, N.; Davis, M. E. Targeting extracellular DNA to deliver IGF-1 to the injured heart. *Sci. Rep.* **2014**, *4*, 4257.
- (12) Dasari, M.; Lee, S.; Sy, J.; Kim, D.; Lee, S.; Brown, M.; Davis, M.; Murthy, N. Hoechst-IR: an imaging agent that detects necrotic tissue in vivo by binding extracellular DNA. *Org. Lett.* **2010**, *12*, 3300–3303.
- (13) Huang, S. N.; Chen, H. H.; Yuan, H. S.; Dai, G. P.; Schuhle, D. T.; Mekkaoui, C.; Ngoy, S.; Liao, R.; Caravan, P.; Josephson, L.; Sosonovik, D. E. Molecular MRI of acute necrosis with a novel DNA-binding gadolinium chelate: kinetics of cell death and clearance in infarcted myocardium. *Circ. Cardiovasc. Imag.* **2011**, *4*, 729–737.
- (14) Perez-Ariza, C.; Busto, N.; Leal, J. M.; Garcia, B. New insights into the mechanism of the DNA/doxorubicin interaction. *J. Phys. Chem. B* **2014**, *118*, 1288–1295.

- (15) Li, N.; Ma, Y.; Yang, C.; Guo, L. P.; Yang, X. R. Interaction of anticancer drug mitoxantrone with DNA analyzed by electrochemical and spectroscopic methods. *Biophys. Chem.* **2005**, *116*, 199–205.
- (16) Kobylecka, M.; Maczewska, J.; Fronczewska-Wieniawska, K.; Mazurek, T.; Plazinska, M. T.; Krolicki, L. Myocardial viability assessment in  $^{18}\text{F}$ FDG PET/CT study ( $^{18}\text{F}$ FDG PET myocardial viability assessment). *Nucl. Med. Rev.* **2012**, *15*, 52–60.
- (17) Osborn, E. A.; Jaffer, F. A. The Advancing Clinical Impact of Molecular Imaging in CVD. *JACC: Cardiovas. Imag.* **2013**, *6*, 1327–1341.